

# Electron-molecule collisions: The influence of microsolvation on the shape resonance spectra and in the differential cross sections

**Márcio H. F. Bettega**

Departamento de Física

Universidade Federal do Paraná

[bettega@fisica.ufpr.br](mailto:bettega@fisica.ufpr.br)

<http://fisica.ufpr.br/bettega>



# Collaborators:



Bruna P. Dias  
Diego F. Pastega  
Thiago C. de Freitas (PhD thesis)



Márcio T. do N. Varella  
Kaline R. Coutinho  
Sylvio R. A. Canuto



UNICAMP

Eliane M. de Oliveira  
Marco A. P. Lima





Curitiba (kur yt yba = many pines)  
 Population: 1.851.215 people  
 (IBGE/2009)

<http://www.curitiba.pr.gov.br/>



# Outline:

- ✓ Motivation.
- ✓ Schwinger multichannel (SMC) method.
- ✓ Applications:  
CH<sub>2</sub>O...H<sub>2</sub>O,  
HCOOH... (H<sub>2</sub>O)<sub>n</sub> (*n*=1,2)  
C<sub>5</sub>H<sub>6</sub>OH... (H<sub>2</sub>O)<sub>n</sub> (*n*=1,2)
- ✓ Conclusions.
- ✓ Acknowledgements.



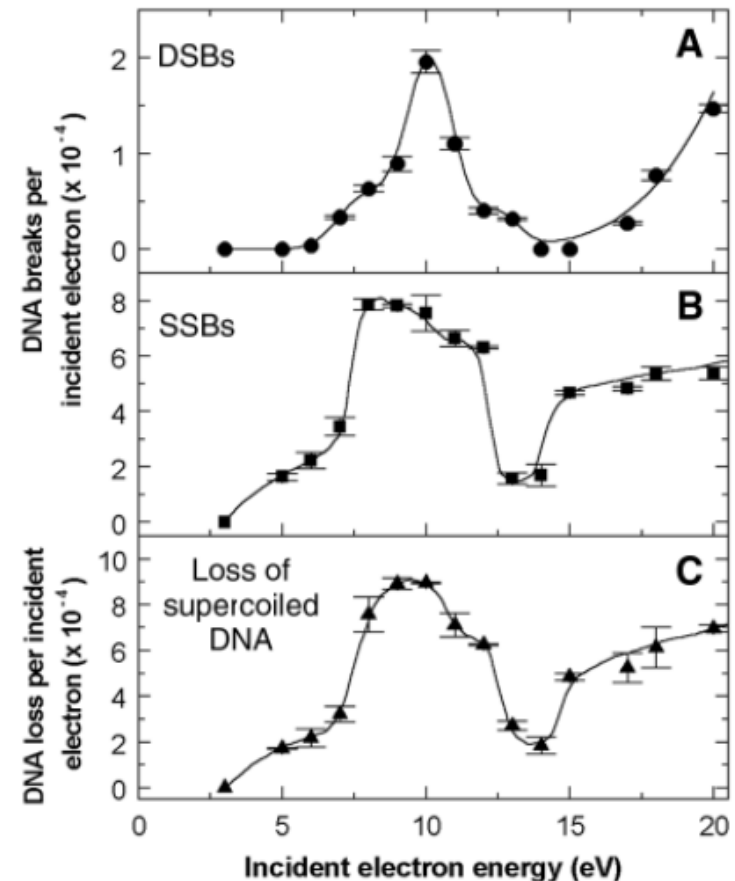
# Motivation:

3 MARCH 2000 VOL 287 SCIENCE 1658

## Resonant Formation of DNA Strand Breaks by Low-Energy (3 to 20 eV) Electrons

Badia Boudaïffa, Pierre Cloutier, Darel Hunting,  
Michael A. Huels,\* Léon Sanche

DNA damage - single- and double-strand breaks in DNA are caused by secondary low-energy (up to 20 eV) electrons generated by the ionizing radiation (X-rays,  $\gamma$ -rays,  $\beta$ -rays).



## Dissociative Electron Attachment to DNA

X. Pan, P. Cloutier, D. Hunting, and L. Sanche\*

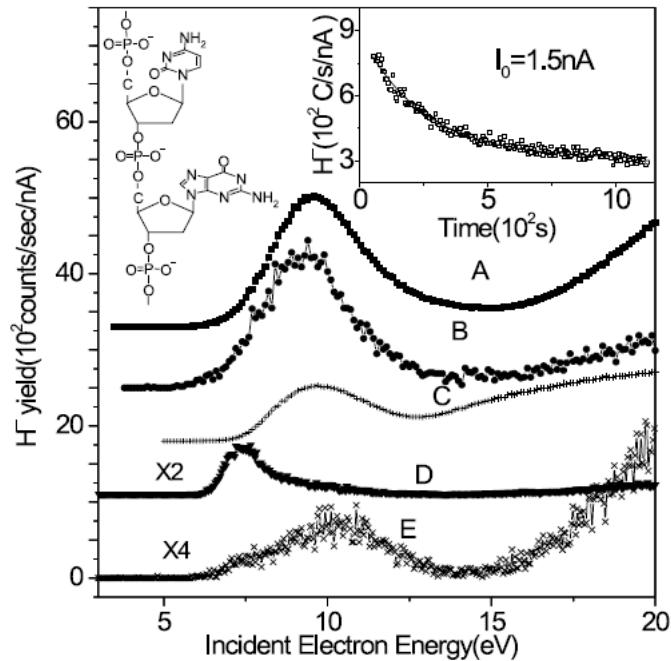


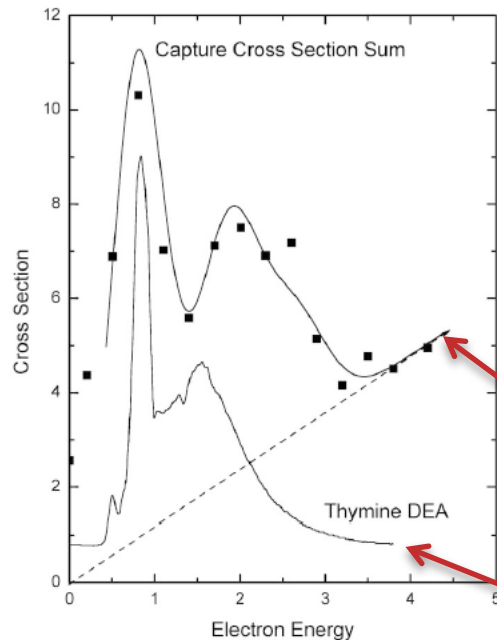
FIG. 1. Incident electron energy dependence of  $H^-$  yields (i.e., the  $H^-$  yield function) from thin films of: (A) double stranded linear DNA, 40 base-pairs, (B) supercoiled plasmid DNA, (C) thymine [6], (D) water [5], and (E) a ribose analog [7]. The zero-count baseline of curves A–D has been displaced for clarity. Part of a single DNA strand is shown in the upper left. The dependence of the magnitude of the  $H^-$  signal on time of exposure to the electron beam is shown by the open squares in the upper right inset. The solid line is an exponential fit to the data.

✓ The formation of  $H^-$ ,  $O^-$  and  $OH^-$  is attributed to dissociative electron attachment (DEA).

✓ "This result further indicates that the measured yields results from a local interaction (e.g., DEA to a basic constituent) not related to the long range geometrical properties of DNA."

## DNA Strand Breaks Induced by 0–4 eV Electrons: The Role of Shape Resonances

Frédéric Martin,<sup>1</sup> Paul D. Burrow,<sup>2</sup> Zhongli Cai,<sup>1</sup> Pierre Cloutier,<sup>1</sup> Darel Hunting,<sup>1</sup> and Léon Sanche<sup>1,\*</sup>



✓ The  $\pi^*$  shape resonances initiate the DEA to DNA.

✓ Results obtained in gas-phase can help in the understanding of processes that occur in condensed phase.

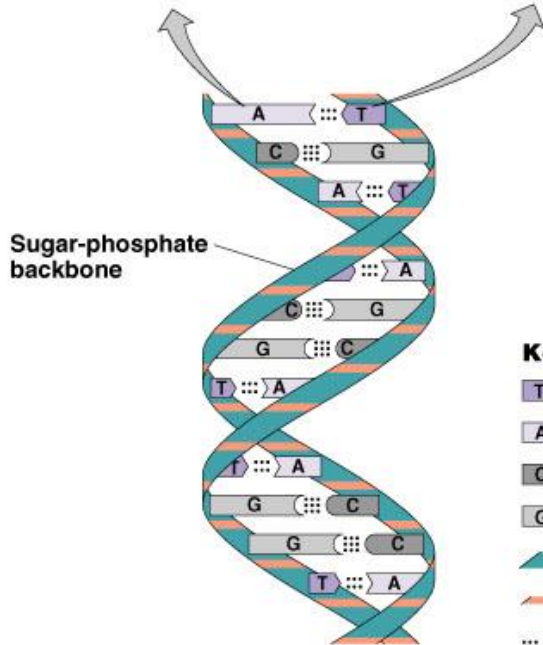
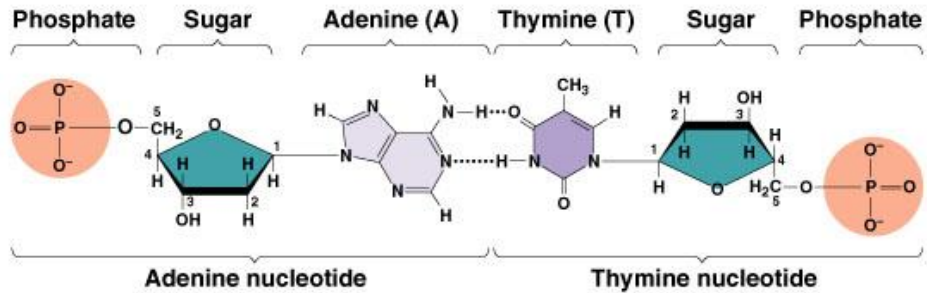
Model using resonances locations  
Computed in gas-phase.

Gas-phase.

FIG. 2. Lower curve: the relative DEA cross section of thymine [10(b)], shifted by 0.2 eV to lower energy. Upper curve: A model of the electron capture cross section of DNA as a function of electron energy based on the resonance energies of the bases and their widths determined in gas-phase scattering studies. The curve has been shifted to higher energy by 0.41 eV, normalized to the SSB data and a linearly increasing background (dashed line) added. Closed squares: SSB yields from Fig. 1.



# Motivation:



DNA double helix

**Key:**

- T Thymine
- A Adenine
- C Cytosine
- G Guanine
- Deoxyribose sugar
- Phosphate
- ... Hydrogen bond

✓ DEA to DNA initiates with the formation of a transient negative ion (shape, core-excited, or Feshbach resonances) → electron-molecule collision problem (gas phase).

✓ Solvation: systems with water.

✓ Gas phase → condensed phase: systems with hydrogen bonds.

Copyright © 2004 Pearson Education, Inc., publishing as Benjamin Cummings.



# The SMC method:

K. Takatsuka and V. McKoy, PRA **24**, 2473 (1981); PRA **30**, 1734 (1984)

- ✓ Extension of the Schwinger variational principle for the scattering amplitude for applications to low-energy electron-molecule collisions;
- ✓ Capable of addressing important aspects of these collisions as:
  - exchange interactions (*ab initio*);
  - effects arising from the polarization of the target by the incident electron (*ab initio*);
  - electronic excitation (multichannel coupling).
- ✓ In the present implementation of the SMC method, to represent the core electrons we employ the local-density norm-conserving pseudopotentials of Bachelet, Hamann and Schlüter [PRB **26**, 4199 (1982)].

M. H. F. Bettega, L. G. Ferreira, and M. A. P. Lima, PRA **47**, 1111 (1993).



# CH<sub>2</sub>O...H<sub>2</sub>O complex:

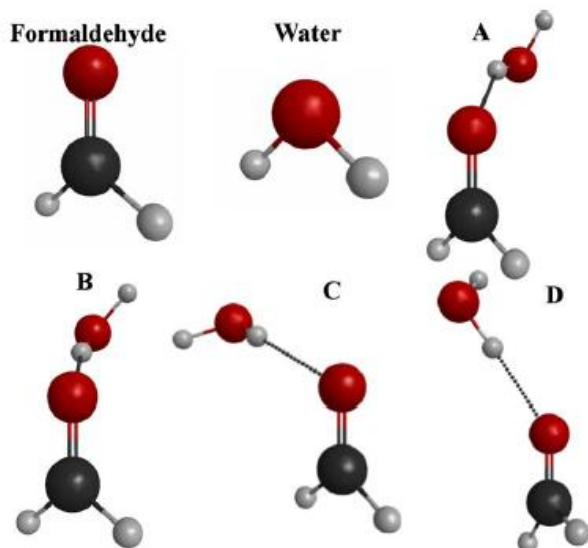
CH<sub>2</sub>O:  $\pi^*$  shape resonance at around 1 eV ( $B_1$ ).

Rescigno *et al.* PRL **63**, 248 (1989); Kaur and Baluja, JPB **38**, 3917 (2005).

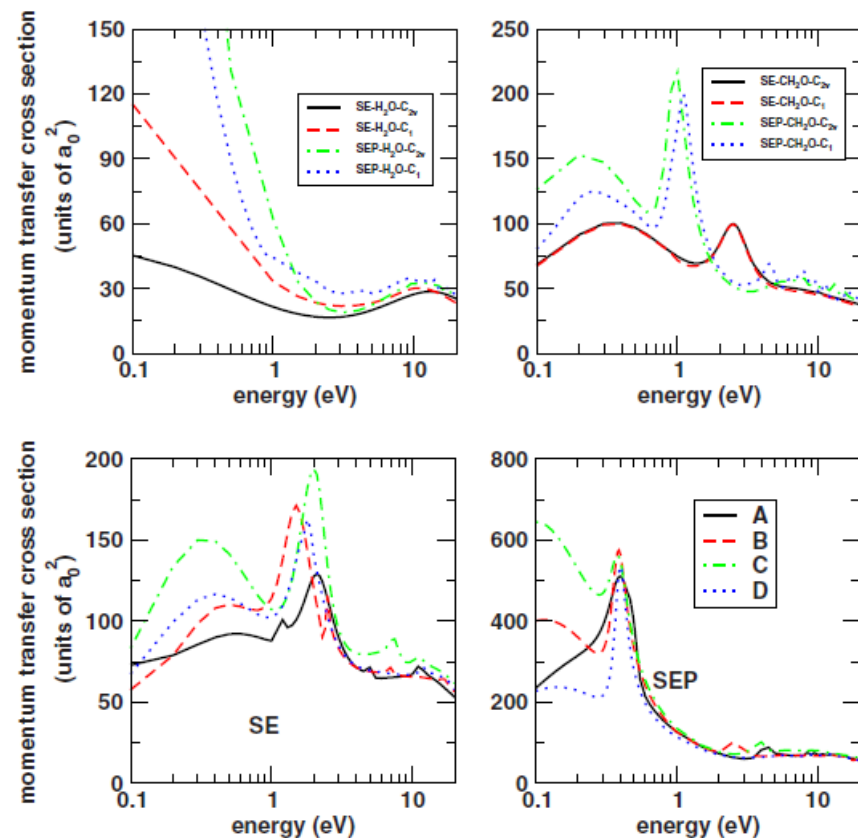
PHYSICAL REVIEW A **80**, 062710 (2009)

## Electron collisions with the CH<sub>2</sub>O-H<sub>2</sub>O complex

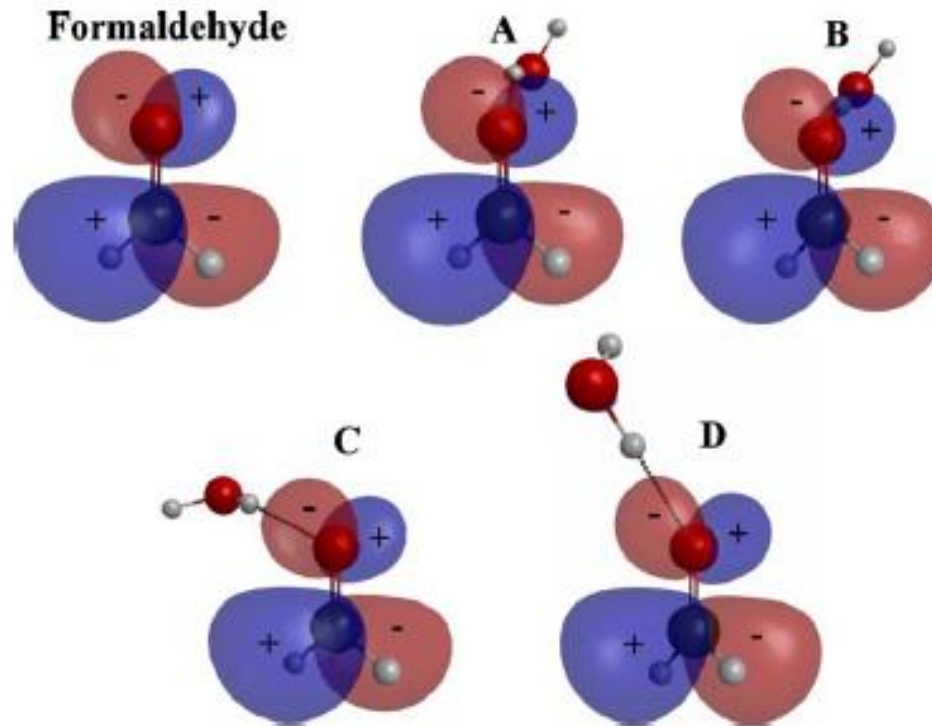
T. C. Freitas,<sup>1,2</sup> M. A. P. Lima,<sup>3,4</sup> S. Canuto,<sup>5</sup> and M. H. F. Bettega<sup>2</sup>



A, B, C, and D: 1W proton donor.  
K. Coutinho and S. Canuto,  
J. Chem. Phys. **113**, 9132 (2000).



# CH<sub>2</sub>O...H<sub>2</sub>O complex:

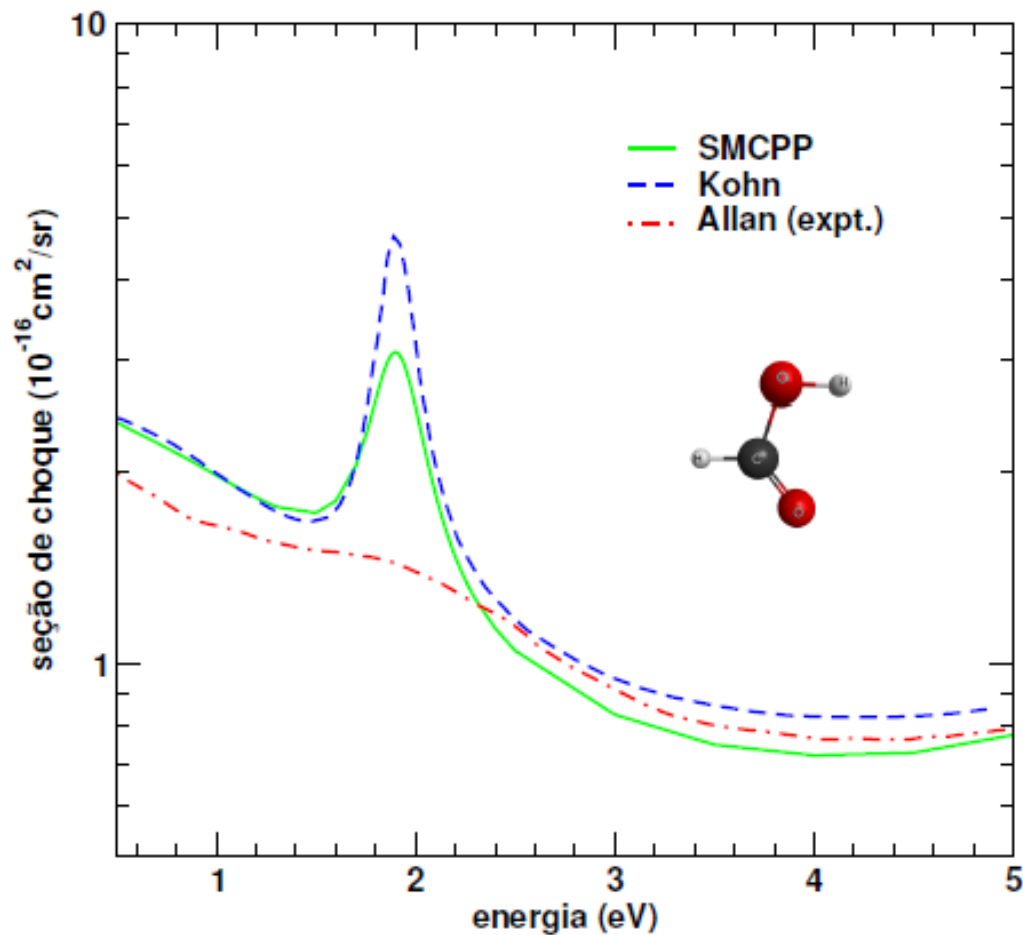


Simulation: the lowest unoccupied orbitals ( $\pi^*$ ) are mostly localized on the solute.

# HCOOH...H<sub>2</sub>O complex:

HCOOH:  $\pi^*$  shape resonance at around 1.9 eV ( $A''$ ).

Pelc *et al.* Chem. Phys. Lett. **361**, 277 (2002); Pelc *et al.* Eur. Phys. J. D **20**, 441 (2002);  
Vizcaino *et al.* New J. Phys. **8**, 85 (2006); M. Allan, J. Phys. B **39**, 2939 (2006);  
Rescigno *et al.* Phys. Rev. Lett. **96**, 213201 (2006); Bettega, Phys. Rev. A **74**, 054701 (2006)



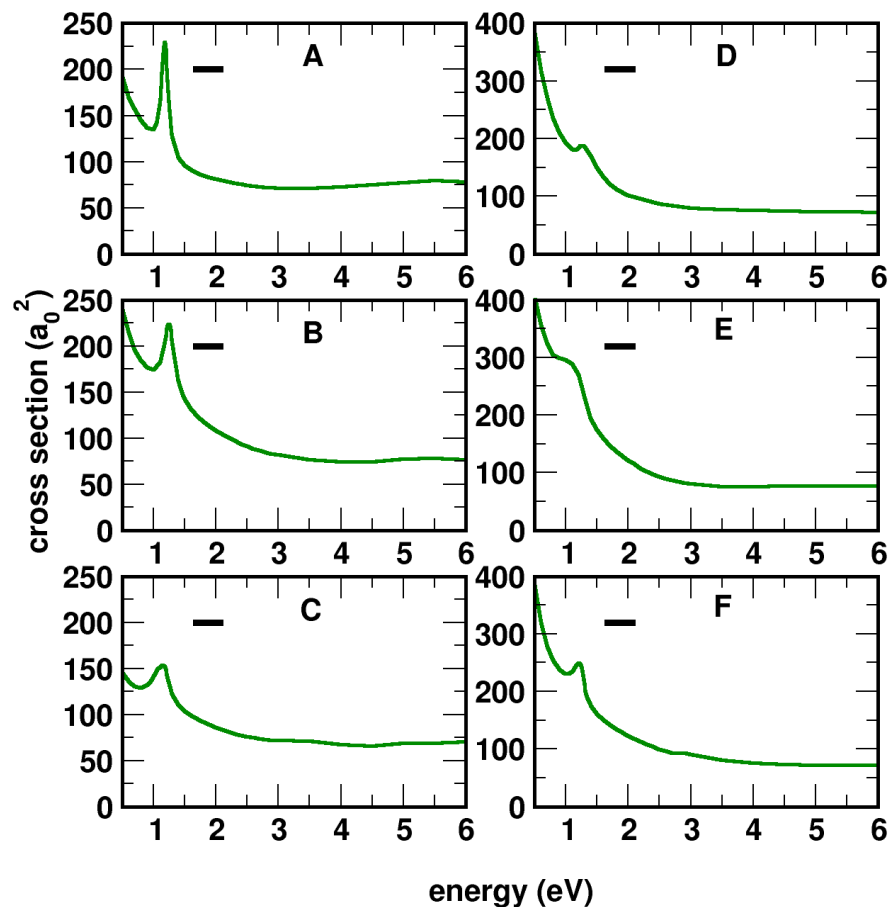
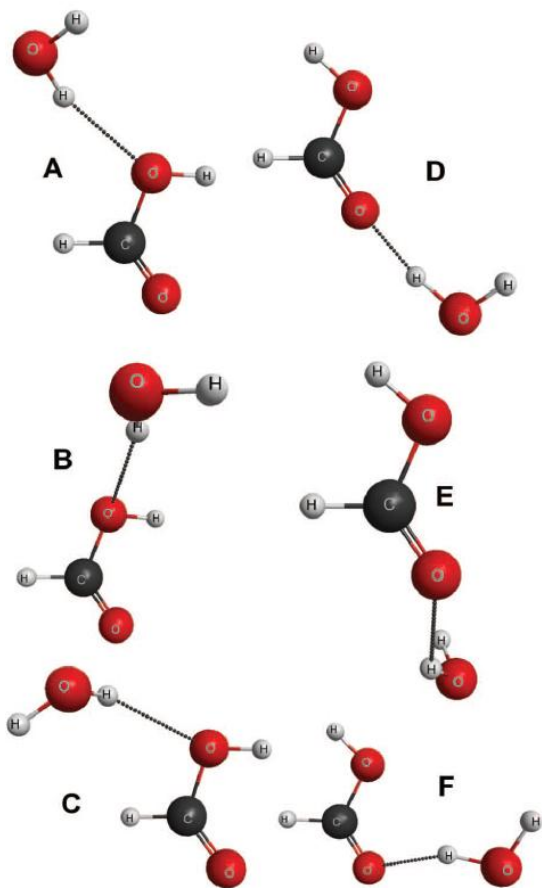
# HCOOH...(H<sub>2</sub>O)<sub>n</sub> complex (n=1,2):

THE JOURNAL OF CHEMICAL PHYSICS 138, 174307 (2013)



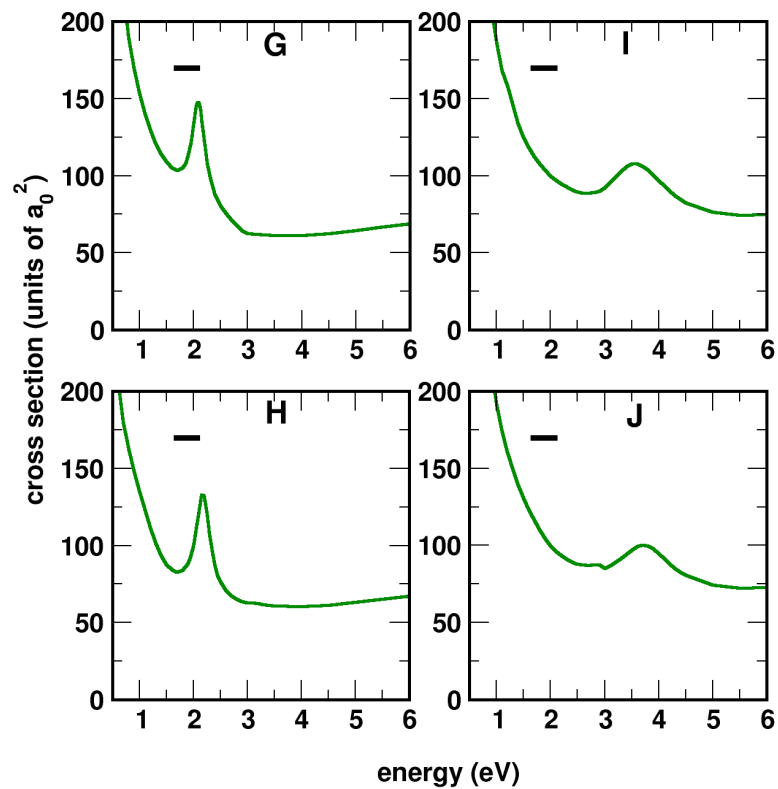
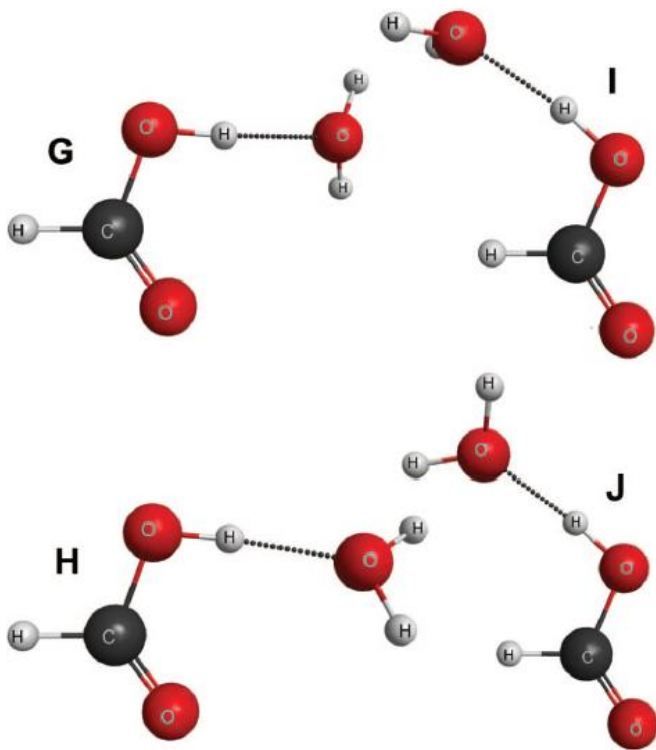
## Electron collisions with the HCOOH... (H<sub>2</sub>O)<sub>n</sub> complexes (n = 1, 2) in liquid phase: The influence of microsolvation on the $\pi^*$ resonance of formic acid

T. C. Freitas,<sup>1,2</sup> K. Coutinho,<sup>3</sup> M. T. do N. Varella,<sup>3</sup> M. A. P. Lima,<sup>4</sup> S. Canuto,<sup>3</sup>  
and M. H. F. Bettega<sup>2,a)</sup>



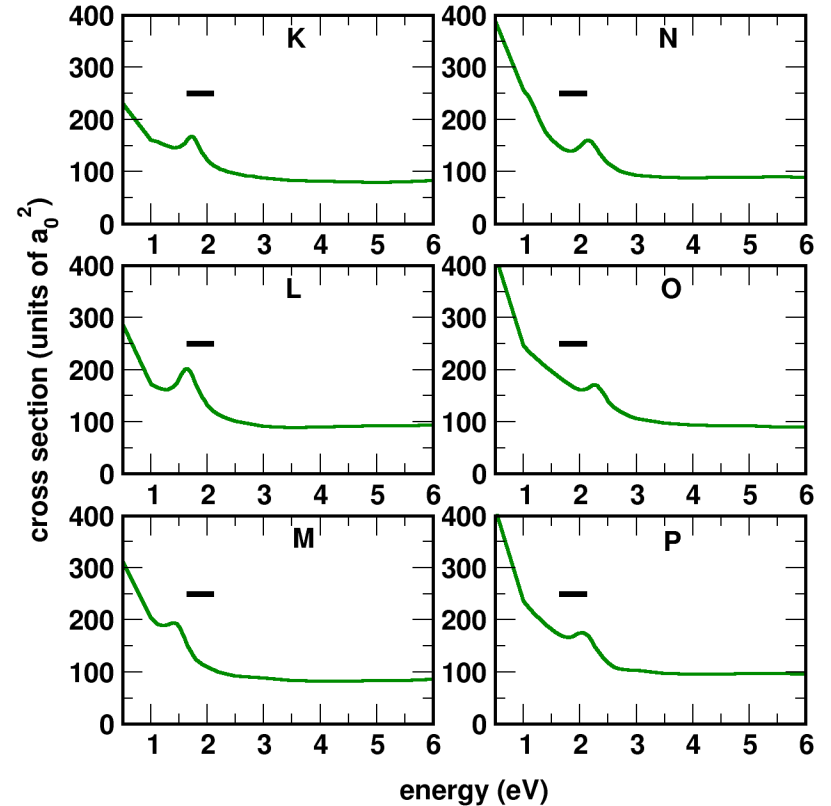
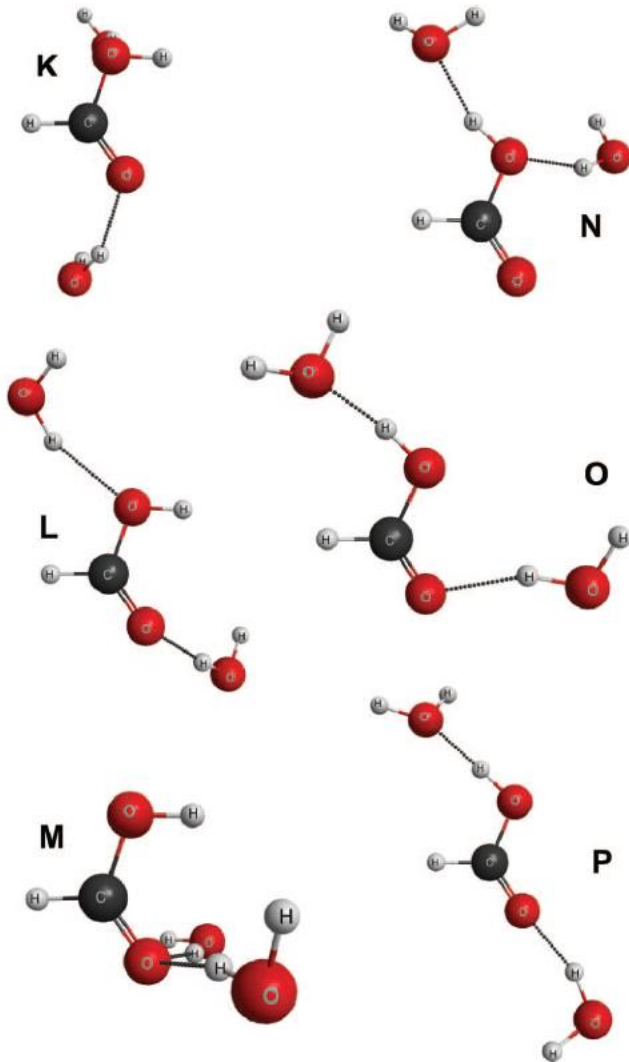
A to F: 1W proton donor.  
A to C: *trans*; D to F: *cis*

# HCOOH...(H<sub>2</sub>O)<sub>n</sub> complex (n=1,2):



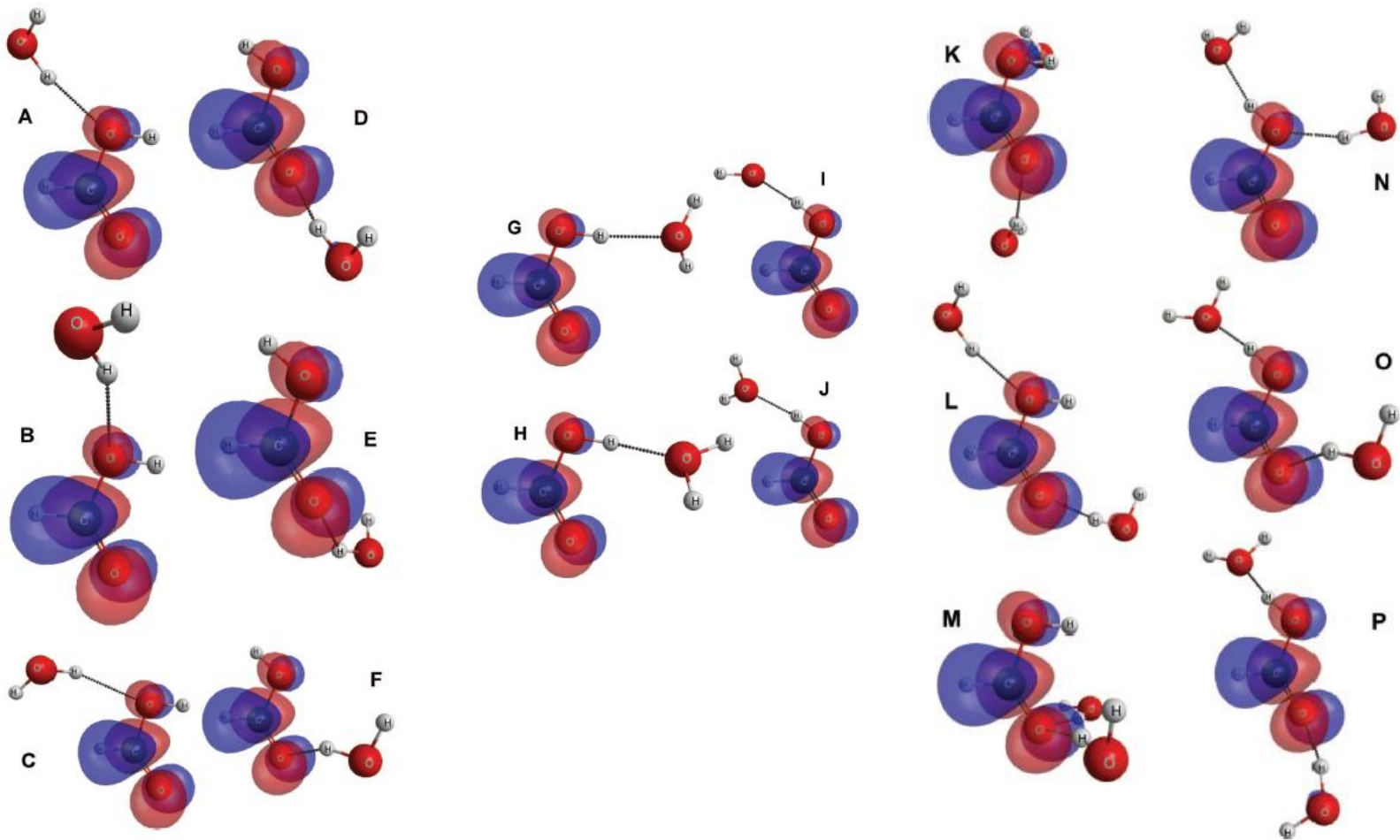
G to J: 1W proton acceptor.  
G and H: *trans*; I and J: *cis*

# HCOOH...H<sub>2</sub>O complex:



K to P: 2W proton donor/acceptor.  
A to C: *trans*; D to F: *cis*

# HCOOH...H<sub>2</sub>O complex:



Simulation: the lowest unoccupied orbitals ( $\pi^*$ ) are mostly localized on the solute.

# HCOOH...H<sub>2</sub>O complex:

TABLE IV. Dipole moment,  $\mu$  (in D), vertical attachment energy, VAE (in units of eV), dipole moment of the formic acid in aqueous solution,  $\mu(\text{HCOOH})_{aq}$ , induce dipole moment due to the aqueous solution,  $\Delta\mu$ , the net charge sign,  $q_{net}$ , and the energy of the resonance peak using the SEP approximation,  $E_r$ . In brackets the experimental values are presented for the dipole moment<sup>46</sup> and the energy of the resonance.<sup>14-24</sup>

	$\mu$	VAE	$\mu(\text{HCOOH})_{aq}$	$\Delta\mu$	$q_{net}$	$E_r$
H <sub>2</sub> O	1.81 [1.85]	5.26				[10.0] ( $\sigma^*$ )
<i>trans</i> -HCOOH	1.42 [1.41]	3.59				1.9 [1.9] ( $\pi^*$ )
<i>cis</i> -HCOOH	3.89	3.59				1.9 ( $\pi^*$ )
A	1.85	3.18	1.94	0.53 (36%)	+	1.2 ( $\pi^*$ )
B	1.49	3.29	1.93	0.52 (36%)	+	1.2 ( $\pi^*$ )
C	1.73	3.32	1.94	0.53 (36%)	+	1.2 ( $\pi^*$ )
D	6.29	2.75	5.45	1.56 (40%)	+	1.2 ( $\pi^*$ )
E	5.92	3.08	5.28	1.39 (36%)	+	1.1 ( $\pi^*$ )
F	6.06	2.99	5.25	1.36 (35%)	+	1.3 ( $\pi^*$ )
G	3.05	4.19	1.95	0.53 (37%)	-	2.1 ( $\pi^*$ )
H	2.65	4.18	1.96	0.54 (38%)	-	2.2 ( $\pi^*$ )
I	6.52	3.80	5.33	1.44 (37%)	-	3.5 ( $\pi^*$ )
J	6.78	3.85	5.33	1.44 (37%)	-	3.7 ( $\pi^*$ )
K	4.43	2.74	2.07	0.65 (46%)	+	1.7 ( $\pi^*$ )
L	3.08	2.37	2.00	0.58 (41%)	+	1.6 ( $\pi^*$ )
M	4.40	2.09	1.95	0.53 (37%)	+	1.5 ( $\pi^*$ )
N	8.00	3.70	5.37	1.48 (38%)	-	2.2 ( $\pi^*$ )
O	9.25	3.84	5.31	1.41 (36%)	-	2.3 ( $\pi^*$ )
P	9.35	3.61	5.41	1.52 (39%)	-	2.1 ( $\pi^*$ )



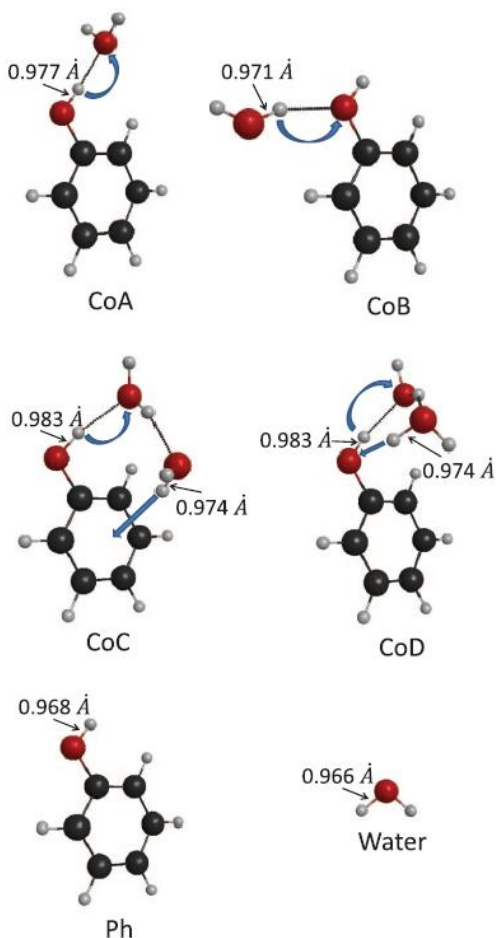
# $C_6H_5OH \dots (H_2O)_n$ complex ( $n=1,2$ ):

THE JOURNAL OF CHEMICAL PHYSICS 141, 051105 (2014)



## Communication: Transient anion states of phenol...( $H_2O$ ) $_n$ ( $n = 1, 2$ ) complexes: Search for microsolvation signatures

Eliane M. de Oliveira,<sup>1</sup> Thiago C. Freitas,<sup>2</sup> Kaline Coutinho,<sup>3</sup> Márcio T. do N. Varella,<sup>3</sup> Sylvio Canuto,<sup>3</sup> Marco A. P. Lima,<sup>1</sup> and Márcio H. F. Bettega<sup>4,a)</sup>



### Geometry optimization

R. C. Barreto, K. Coutinho, H. C. Georg, and S. Canuto, *Phys. Chem. Chem. Phys.* **11**, 1388 (2009).



# $C_6H_5OH...(H_2O)_n$ complex ( $n=1,2$ ):

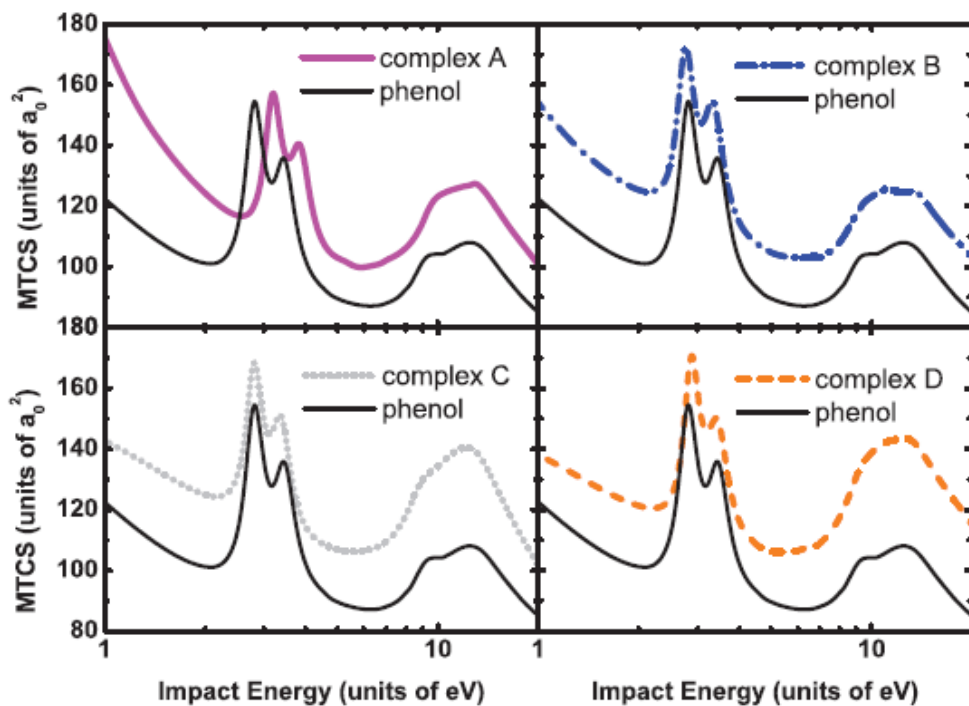
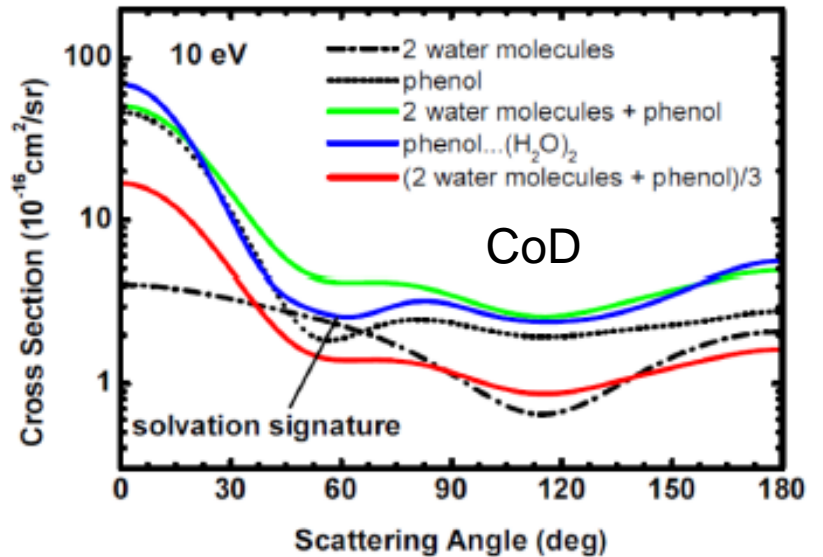
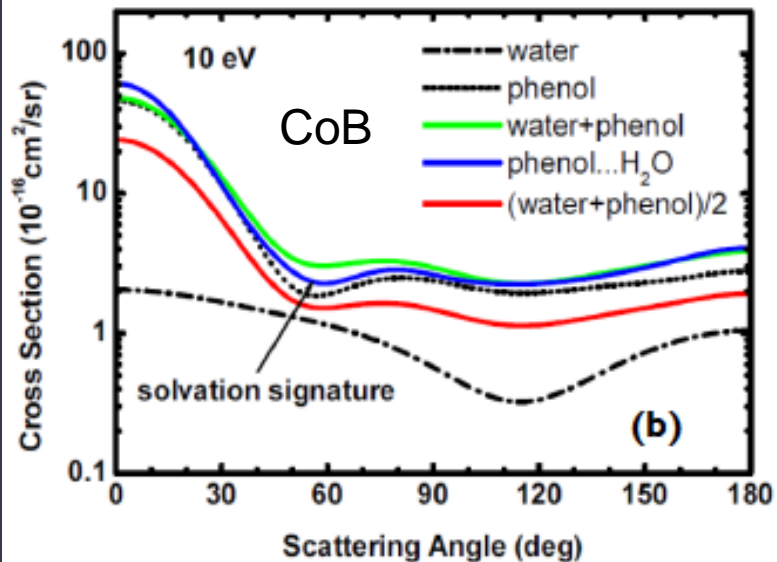
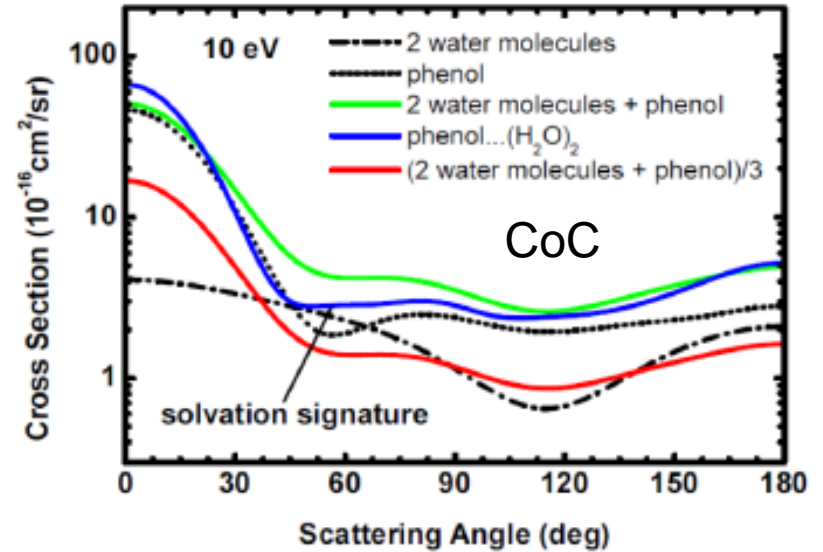
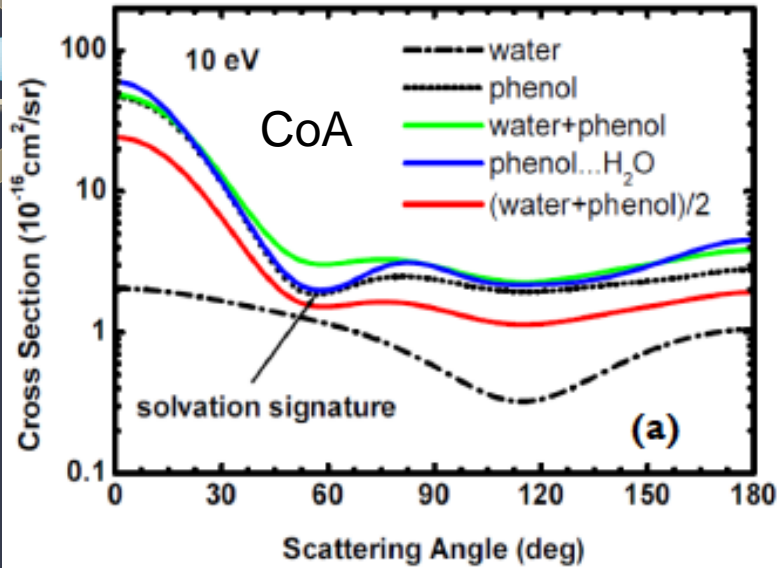


TABLE I.  $\pi^*$  resonance positions ( $E_{res}$ ) and widths ( $\Gamma$ ), in units of eV, for phenol and the phenol...( $H_2O$ ) $_n$  complexes, with  $n = 1, 2$ , shown in Fig. 1. The resonance parameters were obtained from fits to the SE-level eigenphase sums.<sup>18</sup>

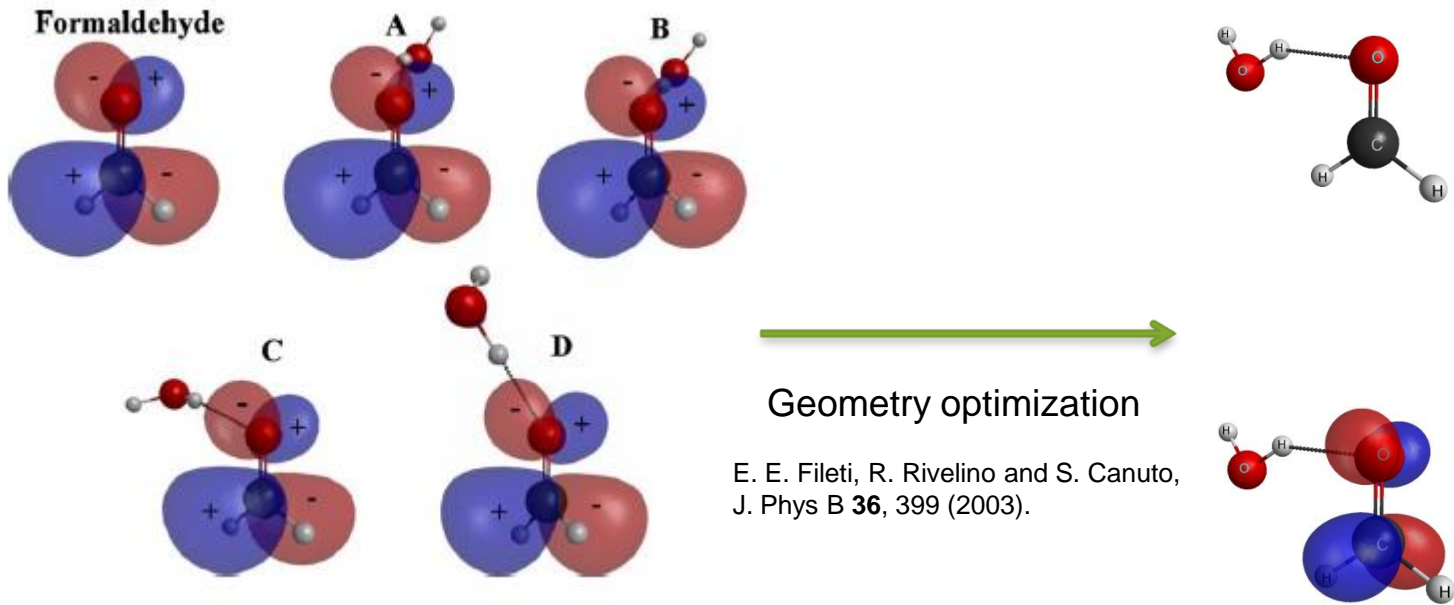
System	$E_{res}(\pi_1^*)$	$\Gamma(\pi_1^*)$	$E_{res}(\pi_2^*)$	$\Gamma(\pi_2^*)$
Phenol	2.81	0.47	3.43	0.60
Complex A	3.20	0.51	3.83	0.64
Complex B	2.74	0.41	3.30	0.60
Complex C	2.81	0.38	3.35	0.58
Complex D	2.82	0.47	3.41	0.64



# $C_6H_5OH... (H_2O)_n$ complex ( $n=1,2$ ):



# CH<sub>2</sub>O...H<sub>2</sub>O complex:



Simulation  
 Lowest unoccupied orbitals ( $\pi^*$ ).

Virtual orbital energies (eV)

A	B	C	D	Opt.	CH <sub>2</sub> O
2.38	1.99	2.21	2.14	2.54	2.85

# Electron-induced hydrogen loss in uracil in a water cluster environment

M. Smyth,<sup>1</sup> J. Kohanoff,<sup>1</sup> and I. I. Fabrikant<sup>2,a)</sup>

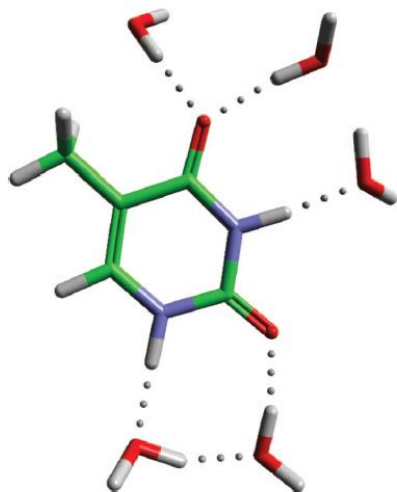


FIG. 2. Illustration of molecular structure of a fully optimized cluster, consisting of one thymine surrounded by five water molecules. The grey balls show hydrogen bonds within the structure.

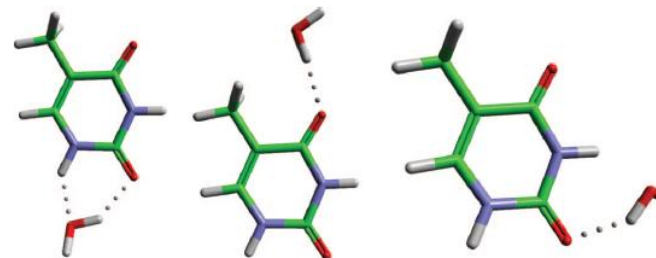


FIG. 3. Optimized structure of each individual water molecule attached to a thymine nucleobase, in configurations A, B, and C, from left to right.

TABLE I. Vertical attachment energies for gas phase thymine, three thymine-single water structures (A, B, and C), and the fully solvated cluster are also given (T+5H<sub>2</sub>O). Energies are calculated using PBE0 and 6-311++G\*\* basis set, and are given in eV.

U/T	1A	1B	1C	5H <sub>2</sub> O
0.435	0.299	0.163	0.218	0.109

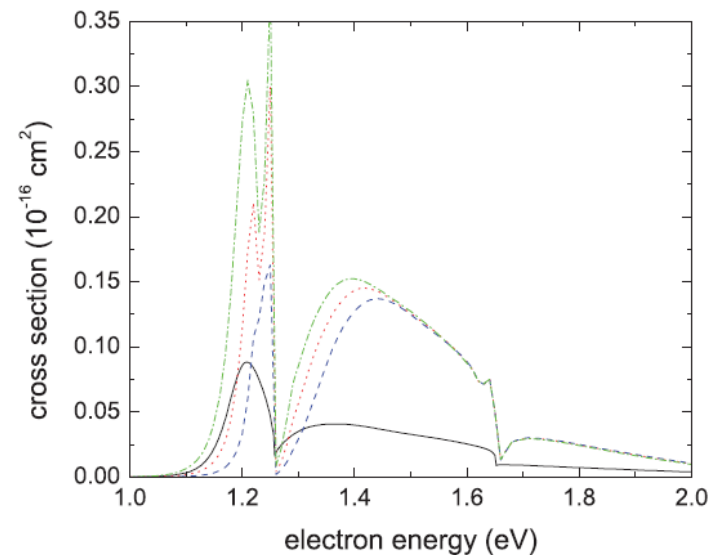


FIG. 6. Dissociative attachment cross section for isolated U/T (black solid curve) and for U/T embedded in the (H<sub>2</sub>O)<sub>5</sub> cluster calculated for three values of the VAE shift  $\Delta E$ : dashed blue,  $\Delta E = 0.04$  eV; dotted red,  $\Delta E = 0$ ; dashed-dotted green,  $\Delta E = -0.04$  eV.

# Conclusions:

- ✓ The presence of water stabilizes(donor)/destabilizes(acceptor) the shape resonance of with respect to the corresponding values in the gas phase (net charge in the solute).
- ✓ The DCSs of a gas of the complexes and of a gas of the independent molecules differ at around  $60^\circ$  suggesting a solvation signature.
- ✓ Geometry optimization: stabilizes (donor)/destabilizes(acceptor) the resonance.



# Acknowledgements:



**FUNDAÇÃO  
ARAUCÁRIA**

**Apoio ao Desenvolvimento Científico  
e Tecnológico do Paraná**



FINANCIADORA DE ESTUDOS E PROJETOS  
MINISTÉRIO DA CIÊNCIA E TECNOLOGIA



Dr. Carlos de Carvalho for computational support at DFis-UFPR and at LCPAD-UFPR.

